



Research Article

Biomaterial Characterization of Decellularized Human Amniotic Membrane Seeded with Fetal Human Cardiac Fibroblasts for Cardiac Tissue Engineering

Firstname Lastname ¹, Firstname Lastname ², Firstname Lastname ^{2,*}

¹Affiliation 1;

²Affiliation 2;

*Corresponding author: e-mail@e-mail.com; Tel.: +xx-xxx; Fax: +xx-xxx

Abstract: The human amniotic membrane (hAM) has emerged as a promising biomaterial in cardiac tissue engineering due to its excellent viability, anti-inflammatory properties, and ability to support cellular adhesion. Its potential as a biomaterial, particularly after undergoing decellularization, offers a novel approach for myocardial regeneration in conditions such as cardiomyopathy and heart failure. We successfully performed the decellularization of hAM using 0.2% (w/v) trypsin/0.25% (w/v) EDTA in phosphate-buffered saline (PBS) depicted by a native epithelial layer of hAM abolishment using hematoxylin-eosin (H&E) staining and ultrastructure analysis. The culture of fetal human cardiac fibroblasts (fHCFs) on decellularized hAM (dehAM) revealed that the fibroblast could attach to the basement membrane of hAM. It maintained its property by expressing a filament marker of vimentin revealed with immunofluorescence. Furthermore, fHCFs cell viability maintained on dehAM was enhanced time-dependent, proving the better proliferation of fHCFs. To the best of our knowledge, this is the first paper that showed the viability of human amniotic membranes with human cardiac resident cells. Our result demonstrates a promising study of dehAM for biomaterial application in cardiac tissue engineering.

Keywords: cardiac fibroblasts; cardiac tissue engineering; cell viability; decellularization; human amniotic membrane.

This work was supported by the Directorate of Research and Development Universitas Indonesia funded by HIBAH PUTI 2022 (NKB 591/UN2.RST/HKP.05.00/2022).

<https://doi.org/xx/ijtech.xx>

Received date; Revised date; Accepted date

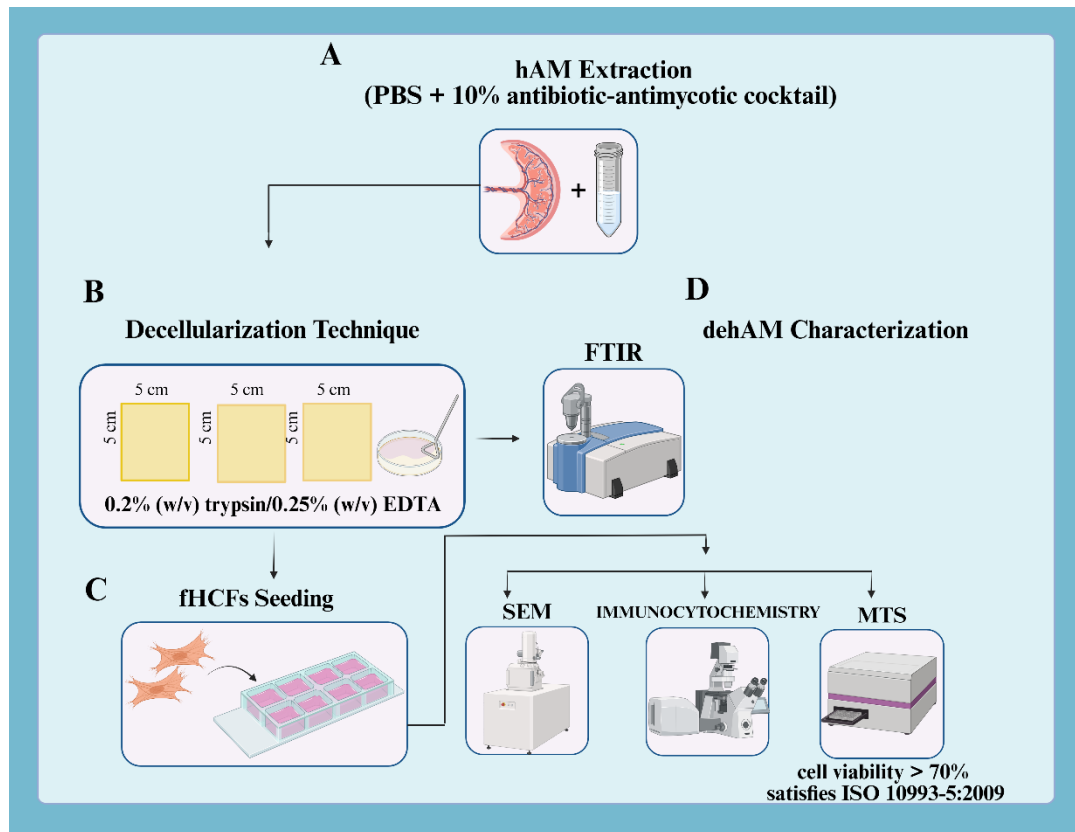


Illustration created with [BioRender.com](https://www.biorender.com/).

1. Introduction

In pediatric patients, heart failure is predominantly caused by congenital heart disease and cardiomyopathy, conditions that lead to detrimental myocardial remodeling characterized by fibrosis (Gordon *et al.*, 2022) (Hsu, 2005). Cardiomyopathy is one of the leading causes of heart transplantation, accounting for 35% of cases (Zhang *et al.*, 2013). The chronic maladaptive process leading to left ventricular remodeling and heart failure in children currently needs ventricular assist devices as bridging therapy before heart transplants, with limited donor availability (Khosravimelal *et al.*, 2020). Such pathological remodeling necessitates innovative therapeutic strategies to restore myocardial function (González *et al.*, 2011). One potential approach is using biomaterial resembling the ECM to create a supportive microenvironment for cardiomyocytes, cardiac fibroblasts, and epithelial cells (Pattar, Hassanabad and Fedak, 2019). Those myocardium resident cells play an important role in remodeling (Wang *et al.*, 2025). However, optimizing biomaterials that have good viability for cellular integration remains a challenge.

The human amniotic membrane (hAM) is a highly valued, naturally derived extracellular matrix (ECM) known for its remarkable biological and regenerative capabilities, making it a popular scaffold in tissue engineering and regenerative medicine (Svystonyuk *et al.*, 2020). Its richness in multipotent stem cells, bioactive molecules, growth factors, and pro-regenerative cytokines promotes re-epithelialization and wound healing across various organs, while also enhancing cell growth, angiogenesis, and vascularization of hAM patches (Moravvej *et al.*, 202;Hu *et al.*, 2023;Solarte David *et al.*, 2022). Beyond these benefits, hAM offers anti-inflammatory, anti-fibrotic, and anti-bacterial properties, alongside excellent viability, low antigenicity, and strong cellular and tissue adhesion, with its composition of elastin fibers, collagen, laminin, hyaluronic acid, and glycosaminoglycans effectively mimicking the natural ECM (Arrizabalaga and Nollert, 2018). Those characteristics make

hAM a promising candidate for biomaterial development, aiming to mimic the ECM and provide a suitable microenvironment for cardiac tissue regeneration (Mamede *et al.*, 2012). Decellularized hAM (dehAM), created by removing the amniotic epithelial cell layer to expose the hAM basement membrane, is widely used in research and clinical applications because it promotes the proliferation, expansion, and differentiation of human bone marrow mesenchymal stem cells (hBM-MSCs) into adipogenic and osteogenic lineages (Salah, Mohamed and El-Badri, 2018). The application of dehAM for cardiac tissue engineering needs to be elucidated before advancing into clinical translational purposes.

The collagen-based hydrogels for tissue engineering have been used in prior studies. Cell viability, viscosity, and syringeability of human bone marrow mesenchymal stem cells (HBM-MSCs) are enhanced on collagen–alginate hydrogels, suitable for injectable applications in tissue engineering (Ketabat *et al.*, 2017). The biocompatibility of HBM-MSCs has been shown on Col/HA hydrogel with highly interconnected porosity. It can be promising for bone tissue engineering (Chen *et al.*, 2017). Previous studies of natural and synthetic polymer fabrication using collagen and alginate with a combination of PVA to develop biomaterial for bone tissue engineering (Fajarani *et al.*, 2024). Furthermore, biomaterial development using a combination of collagen and alginate as a natural polymer showed potential cardioprotective biomaterial by adding propolis as a therapeutic agent (Pangesty *et al.*, 2025). Another study demonstrated the potential of cardio-gel and collagen I for cardiac tissue engineering. This hydrogel has been shown to enhance human foreskin fibroblasts (hFFs) cell viability and cell retention (Khodayari *et al.*, 2024). However, to date, no published studies have investigated resident cardiac cells-based therapy on dehAM for cardiac tissue engineering.

Cardiac fibroblasts, a key resident cell in the myocardium, form a complex 3D network within the connective tissue matrix and establish extensive anatomical contacts with cardiomyocytes (Hall *et al.*, 2021). These cells are vital for both the structure and function of the myocardium, contributing to its structural, biochemical, mechanical, and electrical properties (Hall *et al.*, 2021). Fetal human cardiac fibroblasts (fHCFs), specifically, are crucial for maintaining cardiac tissue homeostasis and facilitating repair (Garate-Carrillo and Ramirez, 2018). Their viability can therefore be used to assess the effectiveness of the amniotic membrane in supporting cardiac tissue. Therefore, investigating the interaction between fHCFs and dehAM holds significant potential for advancing future applications in cardiac tissue engineering. To the best of our knowledge, this is the first study to characterize fetal human cardiac fibroblasts (fHCFs) seeded onto dehAM. This study aims to characterize the fHCFs-dehAM ultrastructure through scanning electron microscopy (SEM), identification of functional group of the dehAM by Fourier transform infrared (FTIR), vimentin expression in the fHCFs-dehAM with immunocytochemistry and cell proliferation of fHCF cells to evaluate the cell viability on dehAM.

2. Methods

2.1 Ethical Clearance

The hAM from donors was procured from healthy pregnant women with negative test results for Hepatitis B, Hepatitis C, HIV, and COVID-19, who underwent elective Caesarean surgery (Moravvej *et al.*, 2021). We acquired signed consent from each participant who agreed to donate their amniotic membrane as per ethical permission approval [IRB/4712/12/ETIK/2022], Institutional Review Board of RSAB Harapan Kita National Women and Children Health Center.

2.2 Preparation of DehAM

The procedure for hAM decellularization was performed using an aseptic technique to maintain stability in a class II Biosafety Cabinet (BSC). Fresh hAM was washed three times with PBS and cut into small pieces of 5 cm x 5 cm. The hAM was separated into two groups for optimization: the first group was incubated in 0.2% (w/v) trypsin/0.25% (w/v) EDTA (Thermo Fisher, USA) at 37°C for 30 minutes, and the second group was incubated in 0.025% (w/v) EDTA at 37°C for 1 hour (Zhang *et al.*, 2013; Khosravimelal *et al.*, 2020). Afterwards, the 0.2% (w/v) trypsin/0.25% (w/v) EDTA group was neutralized with 10% fetal bovine serum (FBS) (Sigma-Aldrich, Cat. F9665) containing Dulbecco's modified Eagle's medium (DMEM) (Sigma-Aldrich, Cat. 12100046), and scraped with a cell scraper to separate residual cells from the membranes. The dehAM morphology is subsequently characterized by H&E staining. The remaining dehAM was stored in 9:1(v/v) FBS:DMSO cryo medium at -80°C.

2.3 Culture of Fetal Human Cardiac Fibroblasts (fHCFs) Cells

The fHCFs were purchased from Cell Application Inc., San Diego, SA. (Cat. 305-05f) and cultured as per the manufacturer's recommendation with slight modification. The cells maintained at density of more than $1 \times 10^4/\text{cm}^2$ in cardiac fibroblast growth medium (CFGF, Cell Application Inc, San Diego, US) with additional supplementation of 15% pre-heated FBS and 1% (v/v) antibiotic-antimycotic (AbAm) cocktail (contains streptomycin, penicillin, and amphotericin) (Sigma-Aldrich, Cat. A5955). Cells were passaged at a confluency of 70–80% to proceed into a further experiment or cryo-preserved in 9:1(v/v) FBS–dimethyl sulfoxide (DMSO) (34943-1L, Sigma Aldrich) stored in a liquid nitrogen tank.

2.4 Seeding fHCFs on DehAM

The dehAM was washed three times in PBS and excised into the size of an 8-well chamber (Thermo Fisher, USA) approximately 10.9 x 8.9 mm or until the well was covered entirely. The fHCFs (8×10^4 cells/well) were seeded onto an 8-well chamber in CFGF-15%FBS as the control group and onto dehAM forming fHCFs-dehAM. The cultures were incubated at 37°C, with 5% CO₂ for 4 ± 2.1 days (expected confluency of 70–80%). The culture was refreshed every three days.

2.5 Characterization Studies

2.5.1 Scanning Electron Microscopy (SEM)

Biomaterial of fHCFs-dehAM were fixated in 2.5% (v/v) glutaraldehyde in deionized water for 1 hour at room temperature. The fixative was removed, and the samples were rinsed three times in PBS before undergoing sequential dehydration in a graded ethanol series (40%, 50%, 70%, 90%, and $2 \times 100\%$ ethanol (v/v) in deionized water, soaked 10 mins each step). Scaffolds were left inside the fume cupboard for 1 hour to complete drying. Samples were stored in a desiccator until use. A Palladium-coated scaffold was assessed by scanning electron microscopy (SEM Evo LS15 Variable Pressure Scanning Electron Microscope, Carl Zeiss, Germany). Secondary electrons were used for imaging purposes at an operating voltage of 5 keV. Compositional analyses were carried out at 15 keV (Caretta *et al.*, 2021; Savić *et al.*, 2021).

2.5.2 Fourier Transform InfraRed (FTIR)

The characterisation of the chemical structures or functional groups of hAM measure with a FTIR test. The concept of principle FTIR works on radiation interference between two rays to produce an interferogram. Infrared spectroscopy rays produce atomic vibrations of a molecule. Infrared spectra are obtained by passing infrared radiation through a sample and determining the fraction of radiation absorbed at a given energy. The energy at each peak in the absorption spectrum appears

according to the vibration frequency of a part of the sample molecule (Stuart 2005). The FTIR spectra of the hydrogels were recorded using a Thermo Scientific Nicolet iN 10 FT-IR Microscope (Thermo Scientific Nicolet iS50, USA). The spectra were recorded from 4000 to 400 cm^{-1} at a resolution of 4 cm^{-1} and 128 scans per sample.

2.5.3 Immunocytochemistry

The fHCFs-dehAM was fixated in 4% paraformaldehyde for 10 minutes and permeabilized with 0.1% Triton X-100 in PBS for 10 minutes. Nonspecific target was blocked with 1% (w/v) bovine serum albumin (Sigma-Aldrich) in PBS for 1 hour, then incubated with 10 $\mu\text{g}/\text{mL}$ mouse anti-human vimentin primary antibody for one hour (MA5-11883, Thermo Fisher, USA) and 2 $\mu\text{g}/\text{mL}$ goat anti-mouse IgG (H+L) secondary antibody for 45 minutes in a dark setup (A21050, Thermo Fisher, USA). Nuclear counterstaining was performed with 10 $\mu\text{g}/\text{mL}$ (v/v) DAPI (Sigma-Aldrich) incubation for 10 minutes. The procedure was conducted at room temperature and washed twice using PBS in between steps (Svystonyuk *et al.*, 2020). The experiment was from 3 independent biological replicates. Images from the fHCFs-dehAM were acquired by Z-stack configuration on Zen 2010 software with confocal laser scanning microscopy (CLSM) 700 (Carl Zeiss, Germany). The excitation laser for DAPI was set at 405 nm and AF633 at 639 nm. The emission signal of AF633 was filtered through Long Pass mode. Data analysis for 2D reconstruction and vimentin-positive fHCFs were performed on ImageJ version 1.54g (Wayne Rasband and contributors National Institutes of Health, USA) software with the Fiji (Wayne Rasband and contributors National Institutes of Health, USA) plugin Bio-Formats and Cell Counter, respectively.

2.5.4 MTS Assay

This study further assesses the viability of fHCF cells on dehAM matrix. A series of cells were grown independently in a flat-bottomed 96-well plate at a density of 1.9×10^4 cells/well in cardiac fibroblast growth medium (CFGF, Cell Application Inc, Cat. 316-500) following culture for 1, 3, and 7 days at 37°C with 5% CO_2 . Cell control was maintained without dehAM, while negative control was to keep only CFG. After incubation, 20 μL of MTS mix solution (CellTiter 96, Promega) was added to each well. Plates were incubated for 2.5 hours in dark conditions at 37°C with 5% CO_2 . Live cell absorbance was read at 490 nm using a microplate reader (Multiskan GO, Thermo Fisher, USA).

2.5.5 Statistical Analysis

The statistical analysis was performed on GraphPad Prism version 10.4.1 for MacOS, GraphPad Software, San Diego, SA, USA. The Shapiro-Wilk test was used to determine data distribution. Two variable data with normal distribution was tested by unpaired Student's T-test, otherwise by Mann-Whitney U test; meanwhile, multiple comparisons from more than two variables were tested by two-way ANOVA with Tukey's multiple comparisons. Data was presented as a standard error of the mean (SEM). Statistically significant value denotes as * $p < 0.05$ significant, ** $p < 0.01$ very significant results, *** $p < 0.001$ highly significant results, and **** $p < 0.0001$ extremely significant results.

3. Results and Discussion

3.1 Decellularization hAM

The placentas were laid on a sterile surgical tray and then thoroughly washed with 0.9% NaCl saline until all blood clots were rinsed down and the membrane showed a light pink color. The amniotic membrane layer was separated from the chorionic membrane by manual separation (Figure 1A), then washed three times with a PBS (MP Biomedicals, Germany) containing 10% antibiotic-antimycotic cocktail (Streptomycin 50 µg/mL, Penicillin 50 µg/mL, and Amphotericin 2.5 µg/mL) and rinsed subsequently three times with sterile PBS, respectively (Figure 1B). We cut the amniotic membrane into squares of approximately 10 x 10 cm² (Figure 1C). The amniotic membrane was then transferred to the laboratory using PBS-contained transport media for further proceedings.



Figure 1. Laboratory workflow on hAM processing from a Cesarean section patient. (A) The separation between the amniotic membrane and chorionic membrane procedure was manually operated in the operation ward. (B) Amniotic membrane pre-treatment with 10% (v/v) AbAm cocktail and rinsed with PBS in a biosafety cabinet adopting aseptic techniques. (C) Procedure of amniotic membrane decellularization with 0.2% (w/v) trypsin/0.25% (w/v) EDTA incorporated with cell scrapping. AM, amniotic membrane; CM, chorionic membrane.

3.2 Evaluation of Decellularization and fHCFs Seeding on dehAM

Cultures of fHCFs were performed on 6-well plates with fHCFs growth medium. Cell culture of fetal human cardiac fibroblasts (fHCFs) using Sigma-Aldrich (Merck) protocol with 15% modified FBS. Cell morphology was examined using an inverted phase microscope to see cell growth. The subculture process was ready to be used for scaffold testing at the 3rd to 8th cell passages.

We performed several tests to determine cell attachment of fHCFs cultured on dehAM using HE staining, SEM, and immunocytochemistry. Visualization of dehAM by H&E staining showed the morphology of dehAM seeded with fHCFs, successful adherence of the seeded cells on the surface of dehAM. An even distribution of spindle-shaped cells with elongated cytoplasm indicated fibroblast adherence after a period of culture maintenance (Figure 2C). The decellularization process demonstrating the complete absence of epithelial cells from the peripheral basement membrane, compared to native hAM (Figure 2A-B).

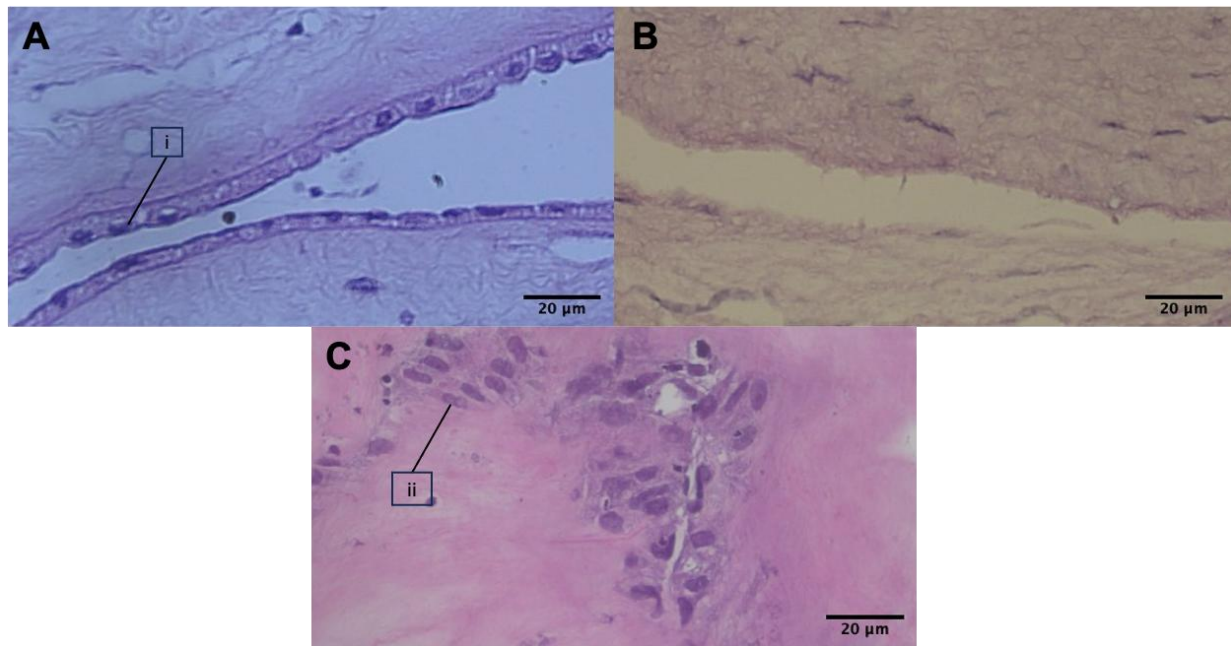


Figure 2. The biocompatibility of the dehAM biomaterial was characterized by fHCFs attachment to the basement membrane. (A) The control group showed the presence of epithelial cells on native hAM (B) dehAM, which no visible epithelial cells with an intact basement membrane, indicating a successful decellularization. (C) fHCFs seeded on dehAM biomaterial showed cells attachment with fibroblast characteristics on the surface of the basement membrane. (i) epithelial cells, (ii) fHCFs cell. Magnification, scale bar: x40, 20µm.

Decellularization of the epithelial layer of hAM aims to suppress immunomodulation, membrane-associated antigens, and soluble proteins, therefore preventing the initiation of a cell-mediated or humoral immune response (Wilshaw *et al.*, 2008; Badylak, Taylor and Uygun, 2011; Crapo, Gilbert and Badylak, 2011). Decellularization techniques such as enzymatic, chemical, and physical methods significantly impact the structural integrity and bioactivity of the scaffold (Sarvari *et al.*, 2022). One study showed that hAM decellularization affected only the epithelial layer, and no observable difference was detected in the ultrastructural characteristics of the compact basement membrane of dehAM compared to that of intact hAM. In addition, bundles of ECM proteins and scattered elastic fibers remained unaffected (Salah *et al.*, 2018). Our study showed successfully decellularization hAM with 0.2% (w/v) trypsin 0.25% (w/v) EDTA.

3.3 Scanning Electron Microscopy (SEM)

We subsequently conducted an ultrastructure test of the fHCFs-dehAM to confirm further topology and integrity of the basement membrane and allogeneic fibroblast reintroduction attachment using SEM analysis. The mosaic of native dendritic-shaped stromal cells was visible in fresh hAM (Figure 3A) (Li *et al.*, 2008) compared to dehAM (Figure 3B) with no lesion on the basement membrane. We also found that spindle-shaped morphology on the surface of the basement membrane of dehAM indicated fibroblast characteristics of fHCFs (Figure 3C). This result indicated the viability of fHCFs in dehAM. However, we did not evaluate the remaining basement membrane and its ECM components. Further study should be conducted focusing on the characterization of dehAM, predominantly its structural properties, and whether the decellularization process impairs its mechanical characteristics.

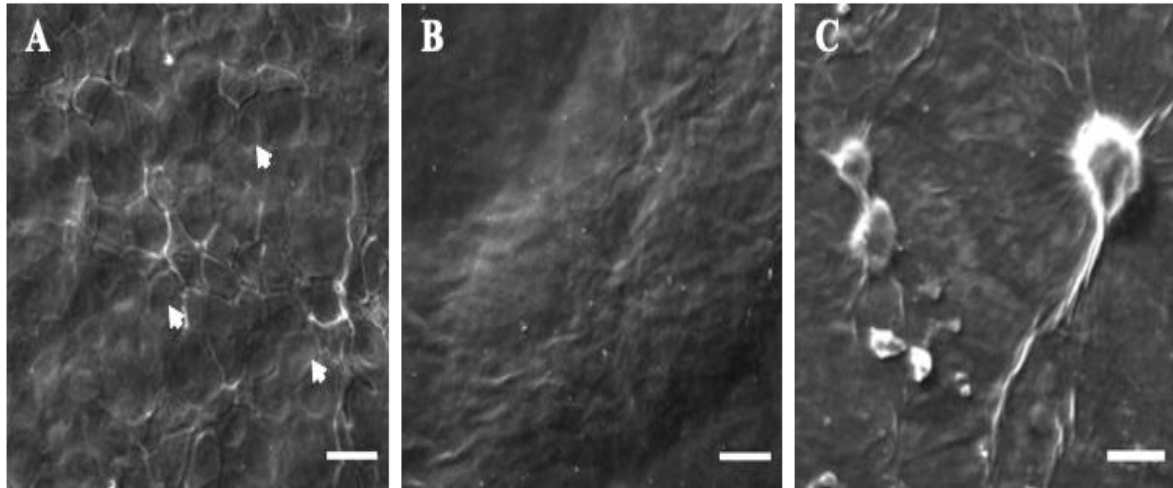


Figure 3. Morphology of dehAM as a biomaterial for fHCFs adherence using SEM analysis. (A) Fresh hAM showed a mosaic arrangement of native epithelial cells (arrowhead); meanwhile, (B) trypsin-treated dehAM successfully denuded the epithelial layer with a compact structure of the basement membrane of dehAM. Magnification 100 \times ; scale bar 20 μm . (C) fHCFs cultured on dehAM biomaterial exhibited spindle-shaped cells, indicating fibroblast adherence on the basement membrane. Magnification 500 \times ; scale bar 40 μm .

3.4 FTIR Molecular Characterization

The FTIR transmittance spectrum of pretreated, native hAM shows the characteristic bands at 3298 cm^{-1} , 1631 cm^{-1} (Skopinska-Wisniewska *et al.*, 2023), and 1079 cm^{-1} (Khalili *et al.*, 2025). The peaks at around 3300–3500 cm^{-1} attributed to N-H/O-H stretching, suggesting the presence of hydroxyl groups of amide (Ji *et al.*, 2020). The peaks at around 1600–1640 cm^{-1} were assigned to the group of amide I and were predominantly attributed to the C=O stretching. The peaks at around 1070–1080 cm^{-1} attributed to PO_2^- stretching, phosphodiester group shows the presence of nucleic acids, phospholipids and glycolipids (Khalili *et al.*, 2025).

After the decellularization process, our study of the FTIR transmittance spectrum of dehAM still shows the amide A (3300 cm^{-1}) and amide I (1630 cm^{-1}) group (Figure 4). Moreover, the spectrum of pretreated, native hAM at 3306.18 cm^{-1} has no significant difference with dehAM at 3310 cm^{-1} (Sripriya and Kumar, 2016). Amide A and amide I are assigned to collagen's hydrogen bonding and structural integrity (Skopinska-Wisniewska *et al.*, 2023). The minimal shift in the peak position of amide A from 3298 cm^{-1} to 3300 cm^{-1} and amide I from 1631 cm^{-1} in pretreated hAM to 1630 cm^{-1} in dehAM, indicating the decellularization process does not alter the collagen structure and maintains extracellular matrix.

Nevertheless, the absence of a phosphodiester group is likely lost during the decellularization process. These changes demonstrate the effectiveness of decellularization in removing cellular components. Based on the result, the decellularization method did not change the chemical properties of the amniotic membrane, which will be decisive in designing the scaffold.

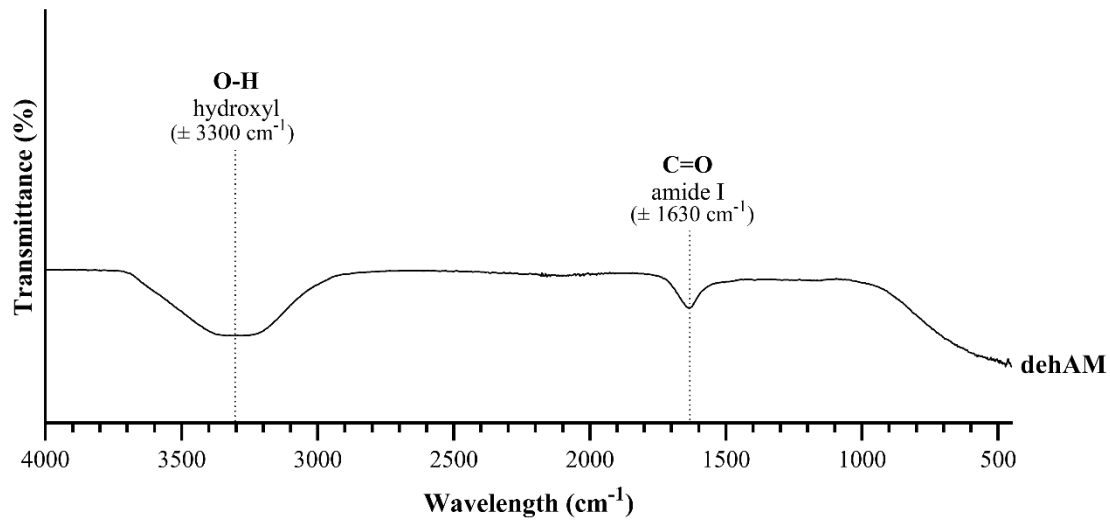


Figure 4. FTIR result showing the functional group present of O-H and C=O stretching.

3.5 Immunocytochemistry

Immunostaining of cells and tissues is widely used as a standard method for the detection of specific targeted proteins, employing antibody binding in conjugation with fluorescence labels. Our results showed that fHCFs in either group had a stereoscopically clear plasma membrane with a long spindle shape, juxtapositioned vimentin organization, and round to oval nuclear (Figure 5A) as previously described (Camelliti et al., 2005). We found that vimentin-positive cells in the fHCFs-dehAM biomaterial complex group had slightly higher numbers than control but not statistically significant, $96.90 \pm 3.2\%$ versus $94.38 \pm 6.0\%$ respectively (Figure 5B).

In our study, fHCF cells maintained their vimentin expression on both the well plate and dehAM matrix. The vimentin expression in fHCFs was approximately 80%, while in fHCFs cultured on dehAM, it showed an increased trend to approximately 90%, although not significant. The numbers of vimentin-positive fHCFs showed no significant difference in either group (Figure 5B), with a slightly higher proportion in fHCFs-dehAM, suggesting that dehAM could support and maintain fHCFs intracellular matrix. Significant differences in vimentin expression were observed across the fHCFs cytoplasm, with intensity measurements revealing notable variations between groups.

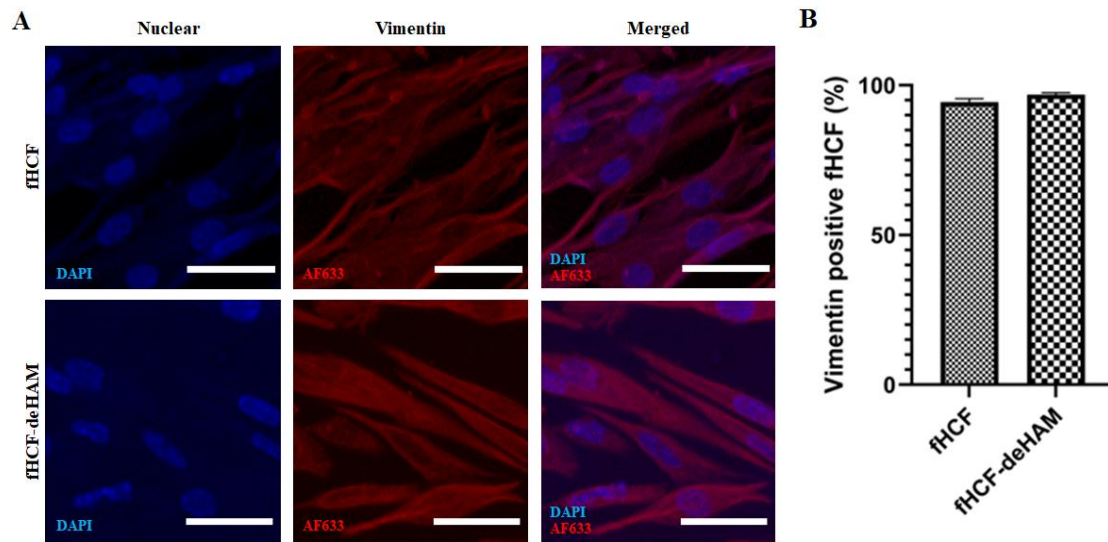


Figure 5. Expression of vimentin in the fHCFs-dehAM was slightly higher but not significantly different. (A) Immunocytochemistry observation using Zeiss confocal laser scanning microscopy (CLSM) 700; fHCFs seeded onto 8-well chamber plasticware as the control group (top panel), and fHCFs-dehAM (bottom panel). Indirect immunofluorescence staining was conducted using anti-vimentin (IgG1) (AF633, red, middle) and nuclear counterstaining (DAPI, blue, left). Magnification, scale bar: x20, 50µm. (B) Quantification of the percentage of vimentin-positive fHCFs between the two groups was compared with the Mann-Whitney U test.

Fibroblast cells cultured on biomaterial could maintain proliferation activity due to collagen presence underpinned adhesive and tensile strength (Taghiabadi *et al.*, 2015). Vimentin played an important role in cellular mechanical integrity and effectiveness of migration (Camelliti *et al.*, 2005). We performed immunocytochemistry to observe the expression of vimentin as a filament marker of cardiac fibroblast as a filamentous protein expressed by mesenchymal cells (Chen and Frangogiannis, 2013). A study about vimentin from fibroblast seeded on dehAM depicted its morphology maintained with positive expression of its marker vimentin and proliferation marker of Ki-67 on a 4-week cultured period (Wilshaw *et al.*, 2008).

Studies have demonstrated that dehAM retains bioactive components that enhance fibroblast proliferation and viability, essential for effective cardiac tissue regeneration (Bahrami *et al.*, 2023). The presence of collagen and laminin in a dehAM supports cell adhesion and survival, ensuring prolonged cellular activity on the scaffold (Hasmad *et al.*, 2022). In vitro studies have demonstrated that hAM extract maintains the original fibroblastic phenotype and reverses differentiated myofibroblasts into fibroblasts (Hu *et al.*, 2023). Another study of Amnio-M showed anti-fibrotic effects by downregulating TGF-β3 and its receptor and suppressing TGF-β transcription and signalling (Elkhenany *et al.*, 2022). The use of dehAM in regenerative medicine became more beneficial because there is no risk of tumorigenicity, decreased inflammation, lower infection, and reduced scar formation (Elkhenany *et al.*, 2022; Hu *et al.*, 2023).

The cytoskeleton structure of the vimentin revealed that the filament distribution expanded throughout the cytoplasm with an interconnected, curvilinear, and smooth structure. Studies on fibroblast cells from various ages and passage stages demonstrated that vimentin expression, measured by intensity, increased with age and passage, with the highest levels seen in cells from

older donors and associated with changes in stiffness and potential glaucoma link (Nishio et al., 2001; Sliogeryte and Gavara, 2019). Vimentin, through its physical properties and signalling pathways, accelerates cell migration regulation and cell attachment to collagen and regulates the formation of cell extensions through connective tissues. Activated vimentin is important in ECM synthesis and remodelling for cellular mechano-protection (Ostrowska-Podhorodecka *et al.*, 2022).

3.6 MTS Assay

The MTS assay was carried out initially with fHCFs seeding on dehAM at 24 hours, 72 hours, and 168 hours. We used a control group which only contained fHCFs medium cultured from well-plate. The relative cell viability of fHCFs cultured on dehAM was recorded at $132.70 \pm 12.01\%$ after 24 hours, $121.15 \pm 5.77\%$ after 72 hours, $72.78 \pm 3.30\%$ after 168 hours. The growth of fHCFs on dehAM was higher at 24 and 72 hours, indicating that fHCFs could adhere to and grow on dehAM. However, at 168 hours, the growth of fHCFs decreased, possibly due to the inability of fHCFs to spread further on the surface of dehAM (Solecki et al., 2024). The result of the MTS Assay can be seen in (Figure 6). The relative cell viability of fHCFs-dehAM compared with fHCFs as control value showed more than 70% in 24, 72, and 168 hours. The cell viability is considered toxic below 70% (Faravelli *et al.*, 2021), which is also based from ISO 10993-5:2009. Therefore, fHCFs-dehAM could be non-toxic and safe for cell growth.

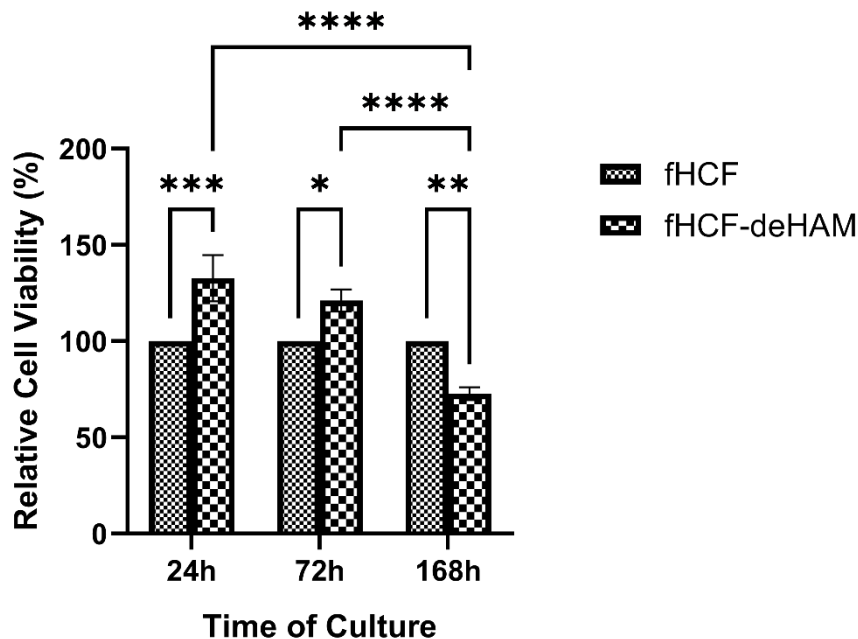


Figure 6. Cell viability of fHCFs on dehAM using the MTS Assay. The analysis was performed using Two-way ANOVA with Tukey's multiple comparisons ($n = 5$ for each group), * ($p < 0.05$) statistically significant, ** ($p < 0.01$) very significant, *** ($p < 0.001$) highly significant, **** ($p < 0.0001$) extremely significant.

The potency of amniotic membrane as an alternative biomaterial had been assessed in various research by MTS assay demonstrating that dehAM supported cell viability in rat brain cells by more than 90% in the first 24 hours of incubation (Susilo *et al.*, 2021). In a study of fibroblasts derived from human neonatal foreskin, tissues were immersed in a trypsin-EDTA solution at 4°C overnight.

Further, the viability and proliferative ability of the fibroblasts seeded on dehAM were evaluated with an MTT assay for 48h, revealing an excellent result. The cell viability in the sample group (amniotic membrane seeded with fibroblast cells) compared to the control groups (fibroblast cells) showed a statistically significant increase until 500% ($P<0.05$). The metabolism activity of viable cells was influenced by growth factors underpinned by the amniotic membrane (Moravvej *et al.*, 2021). An in vitro study about PVA/gelatin hydrogel loaded with propolis has evaluated cytotoxicity using an MTT assay for human embryonic kidney (HEK) 293 cells (Pangesty *et al.*, 2024). The study about stem cells using Wharton's jelly mesenchymal stem cells showed a good differentiation capacity into adipocytes, chondrocytes, and osteocytes for tissue engineering (Rizal *et al.*, 2020). Another in vitro study about biomaterial from umbilical cord blood serum and platelet-rich plasma as coating materials for Poly(ϵ -caprolactone), showed an excellent result for its viability and attachment of human primary fibroblast cells (Nurhayati *et al.*, 2023).

The ECM of freeze-thawed hAM consistently suppresses TGF- β and its receptor at both transcriptional and protein levels in various fibroblast cell types from ocular tissues, even in the presence of exogenous TGF- β (Hu *et al.*, 2023). This suppressive effect is evidenced by the observed downregulation of α -smooth muscle actin transcript expression, a key myofibroblast differentiation marker, within the initial 24 hours of fibroblast culture on hAM, persisting significantly until day 7 in the presence of FBS (Craig *et al.*, 2024). Furthermore, direct contact between fibroblasts and the hAM's basement membrane ECM effectively suppresses TGF- β isoform expression and its co-regulation of α -smooth muscle actin, thereby reducing the potential for scarring in clinical hAM transplantation (Bray *et al.*, 2012). Consequently, the freeze-thawed hAM matrix demonstrates significant promise in attenuating scarring in future translational research, offering compelling implications for clinical applications (Tsen *et al.*, 1999; Nagpal *et al.*, 2016).

The limitation of this study is that the viability assay only showed indirect metabolic activity despite its biocompatibility. We did not perform DNA analysis of the epithelial cells of the amniotic membrane. The human amniotic membrane (hAM) is a promising biomaterial for cardiac tissue engineering due to its biocompatibility and regenerative potential. We suggest using human amniotic membrane-derived mesenchymal cells from the placenta to study myocardial injury *in vivo* or *in vitro* (Maleki *et al.*, 2019) or human induced pluripotent stem cells (Zhou *et al.*, 2019). Further research needs to combine dehAM with hydrogel-based suitable synthetic polymer fabricated into a composite scaffold to develop cardiac tissue engineering (Wang *et al.*, 2021). We also suggest that cell culture technology using a bioreactor has become a better system of 3D cell culture due to being controlled automatically and remotely using multichambers that allow the inflow of fresh liquid or output for sample collection (Irsyad *et al.*, 2022).

4. Conclusions

This study showed that the dehAM is a non-toxic and effective bioscaffold for cardiac tissue engineering. SEM results showed ultrastructure morphology on the dehAM's surface and spindle-shaped fibroblast characteristics. FTIR results showed that physical cross-links provided a stable matrix for the bioscaffold and showed the efficacy of the decellularization method. Immunocytochemistry revealed that dehAM could maintain filament markers of vimentin, demonstrating their stability and functionality while embedded in the bioscaffold. MTS assay showed good viability of dehAM seeded with fHCFs. This study indicates that dehAM is non-toxic and has good cell viability as a potential biomaterial for cardiac tissue engineering.

The dehAM is emerging as a promising biomaterial in cardiac tissue engineering due to its natural and sustainable biomaterial sourced from the human placenta. The dehAM is well-known for fostering cell attachment, proliferation, and tissue regeneration, making dehAM an attractive material for clinical study for cardiac patches and injectable scaffolds. Long-term in vivo studies can provide critical insights to evaluate the safety, efficacy, and potential immunological responses associated with dehAM scaffolds for cardiac tissue engineering.

Continuous research and development are essential to optimized dehAM scaffold innovations for specific cardiac tissue engineering applications. Optimizing the mechanical properties of dehAM, along with FTIR and SEM for thorough characterization, is crucial for advancing their application in cardiac tissue engineering. These efforts will contribute to developing more effective and biomimetic scaffolds for heart repair. Advancements in fabrication techniques, such as electrospinning and melt electrowriting, enable the creation of dehAM scaffolds with controlled mechanical properties and microstructures. Incorporating bioactive molecules or cells into these scaffolds can further enhance their functionality.

Integrating fHCFs into deHAM scaffolds may facilitate the development of functional cardiac tissue constructs. FHCFs can be directed toward a reparative phenotype, promoting tissue regeneration and vascularization. Future research should focus on optimizing scaffold designs and developing strategies to enhance cell retention and survival post-implantation, paving the way for effective cardiac tissue engineering solutions.

Acknowledgements

This study was funded by the Directorate of Research and Development, Universitas Indonesia, under HIBAH PUTI 2022 (Grant No. NKB 591/UN2.RST/HKP.05.00/2022).

Author Contributions

W.A.: conceptualization, methodology, software, formal analysis, resources, data curation, writing – original draft preparation, writing – review & editing. **D.A.C.:** methodology, validation, formal analysis, investigation, data curation, writing – original draft preparation. **A.D.G.:** methodology, validation, formal analysis, writing – original draft preparation. **A.P.K.:** methodology, validation, investigation, writing – original draft preparation. **G.O.:** methodology, writing – original draft preparation, visualization. **R.N.I.:** methodology, writing – original draft preparation. **A.B.:** writing – review & editing. **F.A.R.:** writing – review & editing. **P.A.K.:** software, writing – review & editing, visualization, supervision. **U.P.:** writing – review & editing, supervision. **M.M.D.:** resources, supervision, project administration, funding acquisition.

Conflict of Interest

The authors declare no conflicts of interest.

Supplementary Materials

Supplementary material data available on request from the corresponding author.

References

- Arrizabalaga, J.H. and Nollert, M.U. 2018, 'Human Amniotic Membrane: A Versatile Scaffold for Tissue Engineering', *ACS biomaterials science & engineering*, vol. 4, no. 7, pp. 2226–2236. <https://doi.org/10.1021/ACSBIMATERIALS.8B00015>.
- Badylak, S.F., Taylor, D. and Uygun, K. 2011, 'Whole-organ tissue engineering: Decellularization and recellularization of three-dimensional matrix scaffolds', *Annual Review of Biomedical Engineering*, vol. 13, pp. 27–53. <https://doi.org/10.1146/annurev-bioeng-071910-124743>.

- 443 Bahrami, N., Ale-Ebrahim, M., Asadi, Y., Barikrow, N., Salimi, A. and Roholah, F., 2023, 'Combined
444 Application of Human Amniotic Membrane Mesenchymal Stem Cells and a Modified PGS-co-PCL Film in an
445 Experimental Model of Myocardial Ischemia-Reperfusion Injury', *Applied biochemistry and biotechnology*,
446 vol. 195, no. 12, pp. 7502–7519, <https://doi.org/10.1007/S12010-023-04446-5>.
- 447 Bray, L.J., Heazlewood, C.F., Atkinson, K., Hutmacher, D.W. and Harkin, D.G., 2012, 'Evaluation of
448 methods for cultivating limbal mesenchymal stromal cells', *Cytotherapy*, vol. 14, no. 8, pp. 936–947.
449 <https://doi.org/10.3109/14653249.2012.684379>.
- 450 Camelliti, P., Borg, T.K. and Kohl, P. 2005, 'Structural and functional characterisation of cardiac
451 fibroblasts', vol. 65, , pp. 40–51, <https://doi.org/10.1016/j.cardiores.2004.08.020>.
- 452 Careta, O., Salicio-Paz, A., Pellicer, E., Ibáñez, E., Fornell, J., García-Lecina, E., Sort, J. and Nogués, C.,
453 2021, 'Electroless palladium-coated polymer scaffolds for electrical stimulation of osteoblast-like Saos-2 cells',
454 *International Journal of Molecular Sciences*, vol. 22, no. 2, pp. 528. <https://doi.org/10.3390/ijms22020528>.
- 455 Chen, L., Wu, Z., Zhou, Y., Li, L., Wang, Y., Wang, Z., Chen, Y. and Zhang, P., 2017, 'Biomimetic porous
456 collagen/hydroxyapatite scaffold for bone tissue engineering', *Journal of Applied Polymer Science*, vol. 134,
457 no. 37, pp. 45271, <https://doi.org/10.1002/app.45271>.
- 458 Chen, W. and Frangogiannis, N.G. 2013, 'Fibroblasts in post-infarction inflammation and cardiac repair',
459 *Biochimica et Biophysica Acta (BBA) - Molecular Cell Research*, vol. 1833, no. 4, pp. 945–953,
460 <https://doi.org/10.1016/J.BBAMCR.2012.08.023>.
- 461 Craig, N.A., Scruggs, A.M., Berens, J.P., Deng, F., Chen, Y., Dvornch, J.T. and Huang, S.K., 2024,
462 'Promotion of myofibroblast differentiation through repeated treatment of fibroblasts to low concentrations of
463 PM2.5', *Environmental Toxicology and Pharmacology*, vol. 105, pp. 104329,
464 <https://doi.org/10.1016/j.etap.2023.104329>.
- 465 Crapo, P.M., Gilbert, T.W. and Badylak, S.F. 2011, 'An overview of tissue and whole organ decellularization
466 processes', *Biomaterials*, vol. 32, no. 12, pp. 3233–3243.
467 <https://doi.org/10.1016/J.BIOMATERIALS.2011.01.057>.
- 468 Elkhenany, H., El-Derby, A., Abd Elkodous, M., Salah, R.A., Lotfy, A. and El-Badri, N., 2022, 'Applications
469 of the amniotic membrane in tissue engineering and regeneration: the hundred-year challenge', *Stem Cell
470 Research & Therapy 2021 13:1*, vol. 13, no. 1, pp. 1–19. <https://doi.org/10.1186/S13287-021-02684-0>.
- 471 Fajarani, R., Rahman, S.F., Pangesty, A.I., Katili, P.A. and Park, D.H., 2024, 'Physical and Chemical
472 Characterization of Collagen/Alginate/Poly(Vinyl Alcohol) Scaffold with the Addition of Multi-Walled Carbon
473 Nanotube, Reduced Graphene Oxide, Titanium Dioxide, and Zinc Oxide Materials', *International Journal of
474 Technology*, vol. 15, no. 2, pp. 332–341, <https://doi.org/10.14716/ijtech.v15i2.6693>.
- 475 Faravelli, S., Campioni, M., Palamini, M., Canciani, A., Chiapparino, A. and Forneris, F., 2021, 'Optimized
476 recombinant production of secreted proteins using human embryonic kidney (hek293) cells grown in
477 suspension', *Bio-protocol*, vol. 11, no. 8, pp. 1–15. <https://doi.org/10.21769/BioProtoc.3998>.
- 478 Garate-Carrillo, A. and Ramirez, I. 2018, 'Embryonary Mouse Cardiac Fibroblast Isolation', *Methods in
479 Molecular Biology*, vol. 1752, pp. 71–79. https://doi.org/10.1007/978-1-4939-7714-7_7.
- 480 González, A., Ravassa, S., Beaumont, J., López, B. and Díez, J., 2011, 'New targets to treat the structural
481 remodeling of the myocardium', *Journal of the American College of Cardiology*, vol. 58, no. 18, pp. 1833–
482 1843. <https://doi.org/10.1016/j.jacc.2011.06.058>.
- 483 Gordon, B., González-Fernández, V. and Dos-Subirà, L. 2022, 'Myocardial fibrosis in congenital heart
484 disease', *Frontiers in Pediatrics*, vol. 10, pp. 965204, <https://doi.org/10.3389/fped.2022.965204>.
- 485 Hall, C., Gehmlich, K., Denning, C. and Pavlovic, D., 2021, 'Complex relationship between cardiac
486 fibroblasts and cardiomyocytes in health and disease', *Journal of the American Heart Association*, vol. 10, no.
487 5, pp. e019338, <https://doi.org/10.1161/JAHA.120.019338>.
- 488 Hasmad, H.N., Bt Hj Idrus, R., Sulaiman, N. and Lokanathan, Y., 2022, 'Electrospun Fiber-Coated Human
489 Amniotic Membrane: A Potential Angioinductive Scaffold for Ischemic Tissue Repair', *International Journal
490 of Molecular Sciences* 2022, vol. 23, no. 3, p. 1743, <https://doi.org/10.3390/IJMS23031743>.

- 491 Hsu, D.T. 2005, 'Chronic heart failure in congenital heart disease', in *Pediatric Heart Failure*. CRC Press,
492 pp. 567–588. <https://doi.org/10.1161/cir.0000000000000352>.
- 493 Hu, Z., Luo, Y., Ni, R., Hu, Y., Yang, F., Du, T. and Zhu, Y., 2023, 'Biological importance of human
494 amniotic membrane in tissue engineering and regenerative medicine', *Materials Today Bio*, vol. 22, p. 100790,
495 <https://doi.org/10.1016/j.mtbio.2023.100790>.
- 496 Irsyad, M., Whulanza, Y., Katili, P.A., Antarianto, R.D., Jasirwan, C.O.M. and Bugtai, N., 2022,
497 'Development of Auto-PIVOT: Automated Platform In Vitro for Cell Tissue Culture', *International Journal of*
498 *Technology*, vol. 13, no. 8, pp. 1651–1662, <https://doi.org/10.14716/ijtech.v13i8.6176>.
- 499 Ji, Y., Yang, X., Ji, Z., Zhu, L., Ma, N., Chen, D., Jia, X., Tang, J. and Cao, Y., 2020, 'DFT-Calculated IR
500 Spectrum Amide I, II, and III Band Contributions of N-Methylacetamide Fine Components', *ACS Omega*, vol.
501 5, no. 15, pp. 8572–8578, <https://doi.org/10.1021/acsomega.9b04421>.
- 502 Ketabat, F. Karkhaneh, A., Mehdiavaz Aghdam, R. and Hossein Ahmadi Tafti, S., 2017, 'Injectable
503 conductive collagen/alginate/polypyrrole hydrogels as a biocompatible system for biomedical applications',
504 *Journal of Biomaterials Science, Polymer Edition*, vol. 28, no. 8, pp. 794–805,
505 <https://doi.org/10.1080/09205063.2017.1302314>.
- 506 Khalili, M., Ekhlasi, A., Solouk, A., Nazarpak, M.H. and Akbari, S., 2025, 'A hybrid scaffold of modified
507 human amniotic membrane with gelatine/dendrimer-protected silver nanoparticles for skin wound healing
508 applications', *RSC Advances*, vol. 15, no. 9, pp. 6902–6913, <https://doi.org/10.1039/d4ra08014a>.
- 509 Khodayari, H., Khodayari, S., Rezaee, M., Rezaeiani, S., Alipour Choshali, M., Erfanian, S.,
510 Muhammadnejad, A., Nili, F., Pourmehran, Y., Pirjani, R. and Rajabi, S., 2024, 'Promotion of cardiac
511 microtissue assembly within G-CSF-enriched collagen I-cardiogel hybrid hydrogel', *Regenerative*
512 *Biomaterials*, vol. 11, pp. rbae072, <https://doi.org/10.1093/rb/rbae072>.
- 513 Khosravimelal, S., Momeni, M., Gholipur, M., Kundu, S.C. and Gholipourmalekabadi, M., 2020, 'Protocols
514 for decellularization of human amniotic membrane', *Methods in Cell Biology*, vol. 157, pp. 37–47.
515 <https://doi.org/10.1016/bs.mcb.2019.11.004>.
- 516 Li, W., He, H., Chen, Y.T., Hayashida, Y. and Tseng, S.C., 2008, 'Reversal of myofibroblasts by amniotic
517 membrane stromal extract', *Journal of Cellular Physiology*, vol. 215, no. 3, pp. 657–664.
518 <https://doi.org/10.1002/jcp.21345>.
- 519 Maleki, S.N., Aboutaleb, N., Nazarinia, D., Beik, S.A., Qolamian, A. and Nobakht, M., 2019, 'Conditioned
520 medium obtained from human amniotic membrane-derived mesenchymal stem cell attenuates heart failure
521 injury in rats', *Iranian Journal of Basic Medical Sciences*, vol. 22, no. 11, pp. 1253,
522 <https://doi.org/10.22038/IJBMS.2019.36617.8722>.
- 523 Mamede, A.C., Carvalho, M.J., Abrantes, A.M., Laranjo, M., Maia, C.J. and Botelho, M.F., 2012, 'Amniotic
524 membrane: From structure and functions to clinical applications', *Cell and Tissue Research*. Springer Verlag,
525 vol. 349, pp. 447–458. <https://doi.org/10.1007/s00441-012-1424-6>.
- 526 Moravvej, H., Memariani, H., Memariani, M., Kabir-Salmani, M., Shoaie-Hassani, A. and Abdollahimajd,
527 F., 2021, 'Evaluation of Fibroblast Viability Seeded on Acellular Human Amniotic Membrane', *BioMed*
528 *Research International*, vol. 1, pp. 5597758, <https://doi.org/10.1155/2021/5597758>.
- 529 Morgan, J.T., Raghunathan, V.K., Chang, Y.R., Murphy, C.J. and Russell, P., 2015, 'The intrinsic stiffness
530 of human trabecular meshwork cells increases with senescence', *Oncotarget*, vol. 6, no. 17, pp. 15362,
531 <https://doi.org/10.18632/oncotarget.3798>.
- 532 Nagpal, V., Rai, R., Place, A.T., Murphy, S.B., Verma, S.K., Ghosh, A.K. and Vaughan, D.E., 2016, 'MiR-
533 125b Is Critical for Fibroblast-to-Myofibroblast Transition and Cardiac Fibrosis', *Circulation*, vol. 133, no. 3,
534 pp. 291–301. <https://doi.org/10.1161/CIRCULATIONAHA.115.018174>.
- 535 Nishio, K., Inoue, A., Qiao, S., Kondo, H. and Mimura, A., 2001, 'Senescence and cytoskeleton:
536 Overproduction of vimentin induces senescent-like morphology in human fibroblasts', *Histochemistry and Cell*
537 *Biology*, vol. 116, no. 4, pp. 321–327. <https://doi.org/10.1007/s004180100325>.

- 538 Nurhayati, R.W., Laksono, A.L., Salwa, A., Pangesty, A.I., Whulanza, Y. and Mubarak, W., 2023, 'The
539 Effect of Umbilical Cord Blood Serum and Platelet-Rich Plasma Coatings on the Characteristics of Poly(ϵ -
540 caprolactone) Scaffolds for Skin Tissue Engineering Applications', *International Journal of Technology*, vol.
541 14, no. 7, pp. 1596–1604. <https://doi.org/10.14716/ijtech.v14i7.6709>.
- 542 Ostrowska-Podhorodecka, Z., Ding, I., Norouzi, M. and McCulloch, C.A., 2022, 'Impact of Vimentin on
543 Regulation of Cell Signaling and Matrix Remodeling', *Frontiers in Cell and Developmental Biology*, vol. 10,
544 pp. 869069, <https://doi.org/10.3389/fcell.2022.869069>.
- 545 Pangesty, A.I., Dwinovandi, C.S., Tarigan, S.J.A.P., Rahman, S.F., Katili, P.A., Azwani, W., Whulanza, Y.
546 and Abdullah, A.H., 2024, 'PVA/gelatin hydrogel loaded with propolis for the treatment of myocardial
547 infarction', *Journal of Science: Advanced Materials and Devices*, vol. 9, no. 3, pp. 100732,
548 <https://doi.org/10.1016/j.jsamd.2024.100732>.
- 549 Pangesty, A.I., Kamila, R.A., Schlumbergerina, A.C.P.B., Faizurriqi, M.D., Fakhri, R.W., Sunarso, S.,
550 Zakaria, M.N., Nuraini, L. and Azwani, W., 2025, 'Propolis-Enhanced Alginate-Collagen Injectable Hydrogel
551 Crosslinked with Calcium Gluconate for Myocardial Infarction Therapy', *International Journal of Technology*,
552 vol. 16, no. 3, pp. 1019. <https://doi.org/10.14716/ijtech.v16i3.7366>.
- 553 Pattar, S.S., Hassanabad, A.F. and Fedak, P.W. 2019, 'Acellular extracellular matrix bioscaffolds for cardiac
554 repair and regeneration', *Frontiers in Cell and Developmental Biology*, vol. 7, pp. 63,
555 <https://doi.org/10.3389/fcell.2019.00063>.
- 556 Rizal, R., Syaidah, R., Evelyn, E., Hafizh, A.M. and Frederich, J., 2020, 'Wharton's Jelly Mesenchymal
557 Stem Cells: Differentiation Capacity Showing its Role in Bone Tissue Engineering', *International Journal of*
558 *Technology*, vol. 11, no. 5, pp. 1005–1014, <https://doi.org/10.14716/ijtech.v11i5.4309>.
- 559 Salah, R.A., Mohamed, I.K. and El-Badri, N. 2018, 'Development of decellularized amniotic membrane as
560 a bioscaffold for bone marrow-derived mesenchymal stem cells: ultrastructural study', *Journal of Molecular*
561 *Histology*, vol. 49, no. 3, pp. 289–301, <https://doi.org/10.1007/s10735-018-9768-1>.
- 562 Sarvari, R., Keyhanvar, P., Agbolaghi, S., Roshangar, L., Bahremani, E., Keyhanvar, N., Haghdost, M.,
563 Keshel, S.H., Taghikhani, A., Firouzi, N. and Valizadeh, A., 2022, 'A comprehensive review on methods for
564 promotion of mechanical features and biodegradation rate in amniotic membrane scaffolds', *Journal of*
565 *materials science. Materials in medicine*, vol. 33, no. 3, pp. 32, <https://doi.org/10.1007/S10856-021-06570-2>.
- 566 Savić, L., Augustyniak, E.M., Kastensson, A., Snelling, S., Abhari, R.E., Baldwin, M., Price, A., Jackson,
567 W., Carr, A. and Mouthuy, P.A., 2021, 'Early development of a polycaprolactone electrospun augment for
568 anterior cruciate ligament reconstruction', *Materials Science and Engineering: C*, vol. 129, pp. 112414.,
569 <https://doi.org/10.1016/J.MSEC.2021.112414>.
- 570 Skopinska-Wisniewska, J., Michalak, M., Tworkiewicz, J., Tyloch, D., Tuszynska, M. and Bajek, A., 2023,
571 'Modification of the Human Amniotic Membrane Using Different Cross-Linking Agents as a Promising Tool
572 for Regenerative Medicine', *Materials*, vol. 16, no. 20, pp. 6726, <https://doi.org/10.3390/ma16206726>.
- 573 Sliogeryte, K. and Gavara, N. 2019, 'Vimentin Plays a Crucial Role in Fibroblast Ageing by Regulating
574 Biophysical Properties and Cell Migration', *Cells*, vol. 8, no. 10, pp. 1164,
575 <https://doi.org/10.3390/cells8101164>.
- 576 Solarte David, V.A., Güiza-Argüello, V.R., Arango-Rodríguez, M.L., Sossa, C.L. and Becerra-Bayona.,
577 2022, 'Decellularized Tissues for Wound Healing: Towards Closing the Gap Between Scaffold Design and
578 Effective Extracellular Matrix Remodeling', *Frontiers in Bioengineering and Biotechnology*, vol. 10, pp.
579 821852, <https://doi.org/10.3389/fbioe.2022.821852>.
- 580 Solecki, L., Fenelon, M., Kerdjoudj, H., Di Pietro, R., Stati, G., Gaudet, C., Bertin, E., Nallet, J., Louvrier,
581 A., Gualdi, T. and Schiavi-Tritz, J., 2025, 'Perspectives on the use of decellularized/devitalized and lyophilized
582 human perinatal tissues for bone repair: Advantages and remaining challenges', *Materials Today Bio*, vol. 30,
583 pp. 101364, <https://doi.org/10.1016/j.mtbio.2024.101364>.
- 584 Sripriya, R. and Kumar, R. 2016, 'Denudation of human amniotic membrane by a novel process and its
585 characterisations for biomedical applications', *Progress in Biomaterials*, vol. 5, no. 3, pp. 161–172.
586 <https://doi.org/10.1007/s40204-016-0053-7>.

- Susilo, R.I., Wahyuhadi, J., Sudiana, I.K. and Rantam, F.A., 2021, 'Cytotoxicity test for the use of freeze-dried amniotic membranes against viability, proliferation, and apoptosis on brain cell culture: An in vitro study', *Interdisciplinary Neurosurgery*, vol. 23, p. 100947, <https://doi.org/10.1016/J.INAT.2020.100947>.
- Svystonyuk, D.A., Mewhort, H.E., Hassanabad, A.F., Heydari, B., Mikami, Y., Turnbull, J.D., Teng, G., Belke, D.D., Wagner, K.T., Tarraf, S.A. and DiMartino, E.S., 2020, 'Acellular bioscaffolds redirect cardiac fibroblasts and promote functional tissue repair in rodents and humans with myocardial injury', *Scientific Reports*, vol. 10, no. 1, pp. 9459, <https://doi.org/10.1038/s41598-020-66327-9>.
- Taghiabadi, E., Nasri, S., Shafieyan, S., Firoozinezhad, S.J. and Aghdami, N., 2015, 'Fabrication and Characterization of Spongy Denuded Amniotic Membrane Based Scaffold for Tissue Engineering Citation: Taghiabadi E, Nasri S, Shafieyan S, Jalili Firoozinezhad S, Aghdami N. Fabrication and characteriza-tion of spongy denuded amniotic membrane based scaffold for tissue engineering Fabrication of Spongy Denude AM Scaffold', *Cell Journal (Yakhteh)*, vol. 16, no. 4, pp. 476, <https://doi.org/10.22074/cellj.2015.493>.
- Tseng, S.C.G., Li, D.-Q. and Ma, A.X. 1999, 'Suppression of Transforming Growth Factor-Beta Isoforms, TGF-Receptor Type II, and Myofibroblast Differentiation in Cultured Human Corneal and Limbal Fibroblasts by Amniotic Membrane Matrix', *Journal of cellular physiology*, vol. 179, no. 3, pp.325-335, [https://doi.org/10.1002/\(SICI\)1097-4652\(199906\)179:3<325::AID-JCP10>3.0.CO;2-X](https://doi.org/10.1002/(SICI)1097-4652(199906)179:3<325::AID-JCP10>3.0.CO;2-X).
- Wang, C., Chai, Y., Wen, X., Ai, Y., Zhao, H., Hu, W., Yang, X., Ding, M.Y., Shi, X., Liu, Q. and Liang, Q., 2021, 'Stretchable and Anisotropic Conductive Composite Hydrogel as Therapeutic Cardiac Patches', *ACS Materials Letters*, vol. 3, no. 8, pp. 1238–1248, https://doi.org/10.1021/ACSMATERIALSLETT.1C00146/SUPPL_FILE/TZ1C00146_SI_001.PDF.
- Wang, X. Yu, S., Xie, L., Xiang, M. and Ma, H., 2025, 'The role of the extracellular matrix in cardiac regeneration', *Heliyon*, vol. 11, no. 1, pp. e41157, <https://doi.org/10.1016/j.heliyon.2024.e41157>.
- Wilshaw, S.P., Kearney, J., Fisher, J. and Ingham, E., 2008, 'Biocompatibility and potential of acellular human amniotic membrane to support the attachment and proliferation of allogeneic cells', *Tissue Engineering - Part A*, vol. 14, no. 4, pp. 463–472, <https://doi.org/10.1089/tea.2007.0145>.
- Zhang, T., Yam, G.H.F., Riau, A.K., Poh, R., Allen, J.C., Peh, G.S., Beuerman, R.W., Tan, D.T. and Mehta, J.S., 2013, 'The effect of amniotic membrane de-epithelialization method on its biological properties and ability to promote limbal epithelial cell culture', *Investigative Ophthalmology and Visual Science*, vol. 54, no. 4, pp. 3072–3081, <https://doi.org/10.1167/iov.12-10805>.
- Zhou, H., Wang, L., Zhang, C., Hu, J., Chen, J., Du, W., Liu, F., Ren, W., Wang, J. and Quan, R., 2019, 'Feasibility of repairing full-thickness skin defects by iPSC-derived epithelial stem cells seeded on a human acellular amniotic membrane', *Stem Cell Research and Therapy*, vol. 10, no. 1, pp. 1-13, <https://doi.org/10.1186/s13287-019-1234-9>.